The formation and destruction of fine-structure by double-diffusive processes

P. F. LINDEN*

Abstract—The formation of layered structure by the imposition of an unstable buoyancy flux on a region containing opposing, uniform gradients of two components is examined. TURNER (*Journal of Fluid Mechanics*, **33**, 183–200, 1968) investigated the formation of layers when a stable salinity gradient is heated from below. The present work is an extension of his, allowing for the presence of a de-stabilizing temperature gradient in the interior of the fluid. Experiments were carried out using two solutes (sugar and salt) as the components contributing to the density field. It is found theoretically, and confirmed by experiment, that the scale of the layers depends on the ratio of the two density gradients in the interior $G\rho$. The layers were observed to form sequentially with increasing distance from the boundary across which the buoyancy flux was applied. The relative contributions of the energy provided by the boundary flux and that stored in the destabilizing component during the formation of the first layer are found to depend on $G\rho$ but not on the magnitude of the boundary flux. When $G\rho = 0$, and there is no destabilizing density gradient, all the energy comes from the imposed flux. As $G\rho \to 1$, the energy from the destabilizing component becomes more important, providing all the energy in the limit. Some observations of destruction of fine-structure are reported. Two kinds were observed. One type was characterized by the vertical migration of an interface to an adjacent one thereby destroying the layer in between. The other kind was identified by a breakdown of an interface *in situ*, apparently resulting from an equalization of the density of the two layers on either side. Finally some brief comparisons with oceanic fine-structure are made.

1. INTRODUCTION

OBSERVATIONS of oceanic fine-structure provided by instruments which record temperature or salinity continuously as functions of depth frequently show layered structure. These layers are characterized by regions of relatively weak temperature and salinity gradients bounded above and below by regions (usually thin in comparison to the layers) of relatively large vertical gradients. Layers are found to have a wide range of vertical scales from 100 m down to 1 cm, and indications are that in some cases the horizontal extent of the layers may be some tens of kilometres. It has been suggested many times (see e.g. TURNER, 1973) that one cause of some of this layering may be double-diffusive convection, which can occur when two stratifying components which diffuse at different rates are suitably distributed in a fluid. In the ocean obvious candidates to drive this kind of convection are heat and salt whose coefficients of

molecular diffusion differ by a factor of 80. Indeed, examples of the formation of layered structure by double-diffusive convection using heat and salt have been provided by the laboratory experiments of TURNER (1967, 1968).

Not all layered structures observed in the ocean are a result of double-diffusive convection. What then are the essential characteristics of layers formed in this way? Probably the most obvious clue is the relationship between the temperature and salinity distributions with depth. They should be geometrically similar in the vertical and their mean vertical gradients must have the same sign, thereby contributing in opposite senses to the vertical density gradient. Such situations are found frequently in the ocean (e.g. NESHYBA, NEAL and DENNER, 1971; TAIT and HOWE, 1971)

---

* Department of Applied Mathematics and Theoretical Physics, University of Cambridge, Silver Street, Cambridge CB3 9EW, England.

and are often associated with layered fine-structure. A closer look at such oceanic records raises the more detailed questions of the formation, duration and scales of the layers, and their effects on the vertical transport of heat, salt and momentum. In general, double-diffusive convection provides an efficient means of vertical transport of heat and salt, and these processes may be important in the large-scale thermohaline circulation of the ocean in affording rapid vertical exchanges of heat and salt in some areas.

In this paper some properties of layers formed from initially smooth vertical gradients are examined in the laboratory. Sugar and salt were used as the two components driving the convection. Although the ratio of the coefficients of molecular diffusion (~ 3) is much less than for heat and salt, it is possible (STERN and TURNER, 1969) to reproduce the phenomena observed in laboratory studies using heat and salt. We restrict ourselves here to the so-called diffusive case; i.e. where, in the oceanographic context, hot, salty water lies underneath cold, fresh water. This is simulated by a solution in which the sugar concentration (saccharinity) decreases with height whilst the salinity increases. This restriction is made for convenience only: a consideration of the finger case is reserved for a later date. A far more important limitation is the constraint of one-dimensionality. Again this is made for the sake of simplicity. In a recent paper, TURNER and CHEN (1974) have shown that two-dimensional effects can form layered structure but, for the time being at least, we shall remain in a more tightly constrained configuration. This will mean that care must be taken when attempting to apply the results presented below to oceanic situations (see HUPPERT and TURNER, 1972).

The particular configuration chosen for study is an extension of that examined by TURNER (1968) (hereafter referred to as I). In his paper Turner describes the formation of layers which are produced when a stable salinity gradient is heated from below. The essential addition of these present experiments is to allow for an initial unstable temperature gradient (simulated by a salt gradient) in the fluid as well. Consequently, the energy required to form the layers can come not only from the boundary flux as in I, but also from the energy stored in the temperature field in the interior of the fluid. The evaluation of the effects of these two energy sources is an important aim of this paper. In the ocean it is believed that this 'interior' energy source may be important in the formation of layers, and the case where the unstable temperature gradient is a significant fraction of the stable salinity gradient (in density units) is the rule rather than the exception. Such a situation would arise, for example, if the existing temperature and salinity distributions were a residue of previous double-diffusive fine-structure which has run down leaving the water in a marginally stable state. Then a fresh influx of heat or salt may provide a trigger to re-establish the layers. The influence of the existing stratification on the reforming of layers is sometimes observed to be quite large. In particular, the time scale for the formation of layers from a run-down state may be much less than that required to produce the layers from smooth gradients in the first place.

The remainder of the paper deals with the details of the experiments and their interpretation. The experimental techniques are standard and are described briefly in Appendix 1. In Sections 2 and 3 the layer formation process is discussed by extending the theory of TURNER (1968) to include an unstable temperature gradient in the interior of the fluid. Results of experiments designed to test the theory are also presented. The relative importance of the boundary and interior energy sources is examined in Section 4. In some experiments layers were also observed to coalesce and in Section 5 some ideas concerning the destruction of fine-structure in this way are discussed.

In order to keep the subsequent discussion general the two components contributing to the convection will be denoted by T and S, with coefficients of molecular diffusion κ_T and κ_S, respectively. In all cases T will denote the faster diffusing component, i.e. $\tau \equiv \kappa_S/\kappa_T < 1$. If z is positive upwards, the diffusive configuration corresponds to $d\alpha T/dz < 0$ and $d\beta S/dz > 0$, where

α and β are the changes in density due to unit change in T and S, respectively.

2. THE FORMATION OF THE FIRST LAYER

a. *Theoretical model*

We restrict attention in this section to the formation of the first layer. It was observed (as in I) that the layers formed sequentially, the first one being adjacent to the boundary across which a buoyancy flux is applied. Consequently, it is convenient to describe the formation of each layer in turn.

Consider the case of a fluid layer containing double gradients of T and S in the diffusive sense (see Section 1), with fluxes of T and S across the top boundary of the layer. The layer is assumed to be infinitely deep and the initial gradients will be taken as constant: see Fig. 1. We denote the
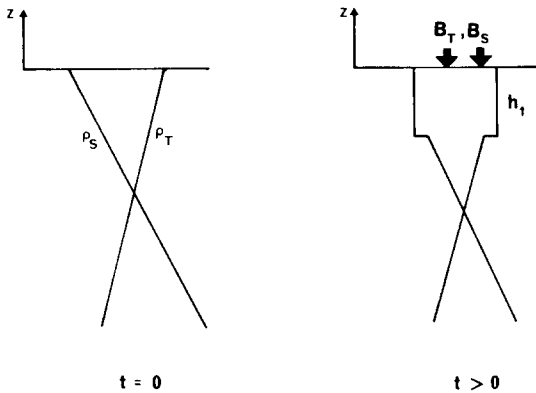
Fig. 1. A representation of the density profiles for the formation of the first layer.

upward buoyancy fluxes of T and S across the top boundary of the layer as $-B_T$ and B_S, respectively. These fluxes are considered to be held constant in time. The buoyancy flux $B_\rho = B_S - B_T$ is negative, thus producing heavy fluid at the top of the gradient region. This heavy fluid produces convection and a mixed-layer of depth $h_1(t)$ is formed.

We need some notation. Let $\rho_{T(S)}$ denote the density anomaly due to $T(S)$, and $\Delta\rho_{T(S)}$ denote the steps in $\rho_{T(S)}$ at the bottom of the mixed layer. We denote the time the boundary fluxes are turned on by $t = 0$. The initial gradients of

T and S in the fluid are given by

$$N_T^2 \equiv -\frac{g}{\bar{\rho}}\frac{d\rho_T}{dz}\bigg|_{t=0} \quad \text{and} \quad N_S^2 \equiv -\frac{g}{\bar{\rho}}\frac{d\rho_S}{dz}\bigg|_{t=0},$$

where $\bar{\rho}$ is a reference density. For the diffusive case under consideration $N_T^2 \leqslant 0$, $N_S^2 \geqslant 0$ and $G\rho = -N_T^2/N_S^2$ takes values in the range $0 \leqslant G\rho \leqslant 1$. The limit $G\rho = 0$ corresponds to the case where there is no unstable distribution of T in the interior of the fluid and describes the conditions of the experiments on heating a stable salinity gradient from below (see I). The limit $G\rho = 1$ corresponds to the situation where the two components contribute equally to the density and there is no overall density gradient in the interior. $G\rho > 1$ implies that the fluid is unstably stratified (i.e. density increases upwards) and this case is excluded: only fluids which are statically stable are discussed.

Following I we now calculate the T and S balance for the layer. For the T balance we note that

$$\rho_T = \rho_0 + \frac{\bar{\rho}}{g}N_T^2 z.$$

Then, with the fact that B_T is independent of time,

$$|\Delta\rho_T| = -\frac{1}{h_1}\int_0^{h_1}\rho_T(z)\,dz + \rho_T(h_1) + \frac{\bar{\rho}}{g}\frac{B_T t}{h_1},$$

$$= -\frac{\bar{\rho}}{2g}N_T^2 h_1 + \frac{\bar{\rho}}{g}\frac{B_T t}{h_1};$$

i.e.

$$\left|\frac{g\Delta\rho_T}{\bar{\rho}}\right| = -\tfrac{1}{2}N_T^2 h_1 + \frac{B_T t}{h_1}. \tag{2.1}$$

Similarly, the S balance for the first layer gives

$$\left|\frac{g\Delta\rho_S}{\bar{\rho}}\right| = \tfrac{1}{2}N_S^2 h_1 + \frac{B_S t}{h_1}. \tag{2.2}$$

A third equation is needed to close the problem. Following I it is assumed that the step in density at the bottom of the mixed layer due to T is proportional to that due to S, i.e.

$$\Delta\rho_T = -k\Delta\rho_S, \tag{2.3}$$

where k is a positive constant, and $k \leqslant 1$ if the

interface is to be statically stable. On energetic grounds it can be shown (see I) that $\frac{1}{3} \leqslant k \leqslant 1$, the lower limit being attained when all the kinetic energy released by the convection is used to mix into the layer and increase its potential energy. In the limit $k = 1$ there is no net density step at the bottom of the layer, the T and S contributions to the density exactly cancelling.

Before manipulating these equations we define one more parameter

$$R_f = -B_S/B_T,$$

the ratio of the buoyancy fluxes of T and S across the top boundary. Then from (2.1), (2.2) and (2.3) we find that

$$h_1 = 2^{\frac{1}{2}} t^{\frac{1}{2}} B_T^{\frac{1}{4}} N_S^{-1}(1+kR_f)^{\frac{1}{4}}(k-G\rho)^{-\frac{1}{4}}, \quad (2.4)$$

$$\left| \frac{g\Delta\rho_T}{\bar{\rho}} \right| = 2^{-\frac{1}{4}} t^{\frac{1}{4}} B_T^{\frac{1}{4}} N_S(1+G\rho R_f)(1+kR_f)^{-\frac{1}{4}}$$
$$\times (k-G\rho)^{-\frac{1}{4}}. \quad (2.5)$$

An immediate consequence of (2.4) is that if layers form in this way $k \geqslant G\rho$. The restriction that the interface be statically stable implies k satisfies

$$G\rho \leqslant k \leqslant 1. \quad (2.6)$$

So far we have dealt only with the time-dependent behaviour of the first layer. It was observed (as in I) that after some time the layer stopped growing and a second layer was formed beneath it. In order to calculate its ultimate depth the model described in I is applied to this situation. The essence of the model is that molecular diffusion of T and S ahead of the advancing layer produces a boundary layer which ultimately becomes unstable, producing convection in a region beneath the first layer. The first layer then stops growing and a second layer is formed. This process will ultimately be responsible for limiting the growth of the second layer and producing a third and so on.

It can be shown (the details are in Appendix 2) that when the T Rayleigh number for this boundary layer of thickness δ_T exceeds a critical value ($\sim 10^3$) then a second layer forms. The Rayleigh number for this boundary layer is given

by

$$R_T = \frac{|g\Delta\rho_T|\delta_T^3}{\bar{\rho}\nu\kappa_T},$$

and we denote the critical value for the onset of convection by R_T^C. It is further shown in Appendix 2 that

$$\left| \frac{g\Delta\rho_T}{\bar{\rho}} \right| = \frac{k}{2} N_S^2 \frac{1+G\rho R_f}{1+kR_f} h_1, \quad (2.7)$$

$$\frac{\delta_T}{h_1} = 2\kappa_T B_T^{-1} N_S^2(1+kR_f)^{-1}(k-G\rho). \quad (2.8)$$

Then using the fact that the depth of the first layer reaches its ultimate value h_1^C when $R_T = R_T^C$ we find that

$$h_1^C = \left(\frac{R_T^C \nu}{4\kappa_T^2} \right)^{\frac{1}{4}} B_T^{\frac{3}{4}} N_S^{-2} k^{-\frac{1}{4}}(1+G\rho R_f)^{-\frac{1}{4}}(1+kR_f)^{-\frac{1}{4}}$$
$$\times (k-G\rho)^{-\frac{3}{4}}. \quad (2.9)$$

Before presenting the experimental results for the formation of the first layer we note some properties of the above equations. We have assumed that B_T and R_f are independent of time. Consequently, (2.4) implies that $h_1(t) \propto t^{\frac{1}{2}}$. The same behaviour was found for the formation of the first layer when a stable salinity gradient was heated from below (I). In fact the only significant difference between the prediction for the depth of the first layer (2.9) and that found in I is the effect of the unstable T distribution represented by the factor $(1+G\rho R_f)^{-\frac{1}{4}}(k-G\rho)^{-\frac{3}{4}}$. This shows that as $G\rho \to k$ the layer will increase in size, ultimately becoming very large in that limit. To test these ideas we now present some of the experimental results.

b. *Experimental results*

One disadvantage of using sugar and salt to model these processes is that it is very difficult to specify the fluxes across the top boundary of the system. By the method described in Appendix 1 of using large steps in T and S at the top of the gradient region an attempt was made to keep B_T and B_S independent of time. Furthermore, to allow comparison from run to run the same steps were used thereby keeping B_T and B_S fixed. The fluxes were provided by diffusive transport across
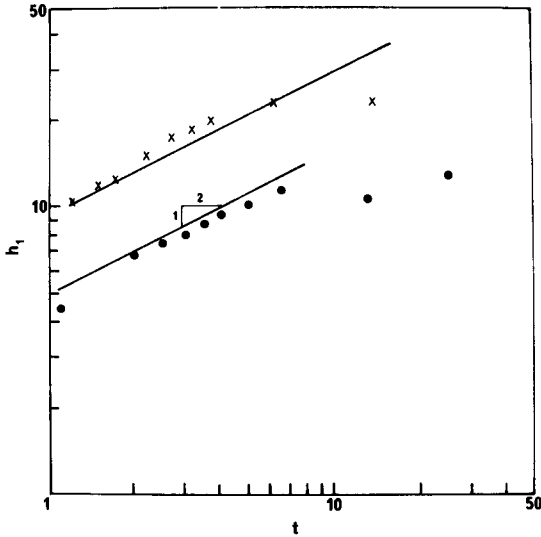
Fig. 2. The depth of the first layer h_1 cm plotted on a log–log scale against the time t min measured from the moment the fluid above the gradient region is added. Shown for comparison with the experimental points are two lines of slope $\frac{1}{2}$.
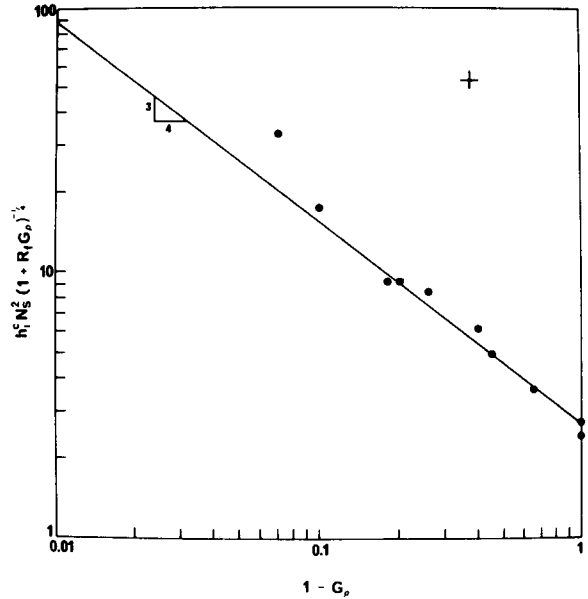
Fig. 3. A log–log plot of the depth of the first layer multiplied by the buoyancy frequency of the S stratification, $h_1^C N_S^2 (1 + R_f G\rho)^{\frac{1}{4}}$ with $R_f = 0.56$, against the ratio of the T and S density gradients $1 - G\rho$. A line of slope $-\frac{3}{4}$ is drawn through the data. Error bars giving estimates of the 90% confidence limits of the data are shown.

an interface at the top of the gradient region and so (SHIRTCLIFFE, 1973) the ratio of the fluxes R_f was also held constant ($R_f \approx 0.6$).

Evidence that the buoyancy fluxes were constant over the majority of the time taken to form the first layer is provided by Fig. 2. The data show the depth of the first layer $h_1(t)$, as determined from a shadowgraph, plotted against the time t after the addition of fluid to the layer above the gradient region. Two lines of slope $\frac{1}{2}$ are shown for comparison. The different h_1 intercepts of the two sets of points reflect the fact that $G\rho$ was different in the two runs.

The dependence of the ultimate layer depth h_1^C on $G\rho$ is shown in Fig. 3. Here we have plotted $h_1^C N_S^2 (1 + G\rho R_f)^{\frac{1}{4}}$ (in arbitrary units) against $(1 - G\rho)$. From (2.9) we would expect that $h_1^C N_S^2 (1 + G\rho R_f)^{\frac{1}{4}} \propto (k - G\rho)^{-\frac{3}{4}}$, when B_T and R_f are constant. Also shown on the figure is a line of slope $-\frac{3}{4}$ and the data are adequately represented by a line of this slope. This good fit provides evidence that $k = 1$, as TURNER (1968)

had found with his experiment using heat and salt. Layers were observed to form for the largest value of $G\rho$ we were able to set up in the laboratory namely $G\rho = 0.96$. Hence (2.6) implies that $0.96 < k < 1$.

Photographs showing the formation of layers in a typical sequence are shown in Fig. 4. Note that each layer is well-mixed and that the interfaces between the layers are very sharp. These interfaces remained sharp over times long compared to the molecular diffusion time of sugar, a feature common in diffusive convection. Although the process appears to be one-dimensional, observations of the flow using time-lapse photography showed that there were often significant horizontal variations in layer thickness and revealed wave motions along the interfaces. However, these motions do not seem to affect the final state of the system, but it is believed that they may in some cases contribute to instabilities which can cause the destruction of an interface (see Section 5).

3. FORMATION OF THE SECOND AND SUBSEQUENT LAYERS

The layers were observed to form consecutively beginning with a layer formed next to a boundary region. This first layer was discussed in the previous section. We now turn to the formation of the second and subsequent layers. There is no reason to expect that the arguments applied to the first layer will not apply to these subsequent layers. However, there is now one significant difference from the first layer. This is that the fluxes at the boundaries of these layers are no longer independent of time, but instead will depend on the steps of T and S across the interface at the top of each layer.

The magnitude of these steps will vary as the new layer forms both as a result of mixing in that layer and due to the flux into the layer immediately above the forming layer. It is then necessary to relate the fluxes of B_T and B_S to the magnitude of the steps, possibly by appealing to models such as those of LINDEN and SHIRTCLIFFE (1977). Then in the manner described in Section 2 the time evolution of a series of layers can be determined. This is a complicated process and beyond the scope of this paper. Instead, we present a much simplified version for the second layer only, in order to estimate some of its properties.

In the simplified model for the formation of the second layer it is assumed that $\Delta\rho_T$ and $\Delta\rho_S$ at the interface between the first and second layer remains constant throughout the formation of the layer. We take values appropriate to those at the beginning of its formation, i.e. $\Delta\rho_T$ has the value reached when the first layer stops growing. Dimensional analysis (LINDEN and SHIRTCLIFFE, 1977) shows that the flux into the layer B_T is given by an expression of the form

$$B_T = f\left(\frac{\Delta\rho_T}{\Delta\rho_S}\right)\left|\frac{g\Delta\rho_T}{\rho}\right|^{4/3}. \qquad (3.1)$$

This form for the flux has been supported by direct measurements (TURNER, 1965; SHIRTCLIFFE, 1973). Now $\Delta\rho_T/\Delta\rho_S = -k = $ constant, and so use of (2.7) and (2.9) gives

$$B_T \propto B_T^0(1 + G\rho R_f)(1 + kR_f)^{-2}(k - G\rho)^{-1}, \qquad (3.2)$$

where B_T^0 is the flux imposed at the top of the first layer. Thus, by analogy with (2.9) the ultimate depth of the second layer h_2^C is given by

$$h_2^C \propto B_T^{0\frac{3}{4}}N_S^{-2}(1 + G\rho R_f)^{\frac{3}{4}}(1 + kR_f)^{-2} \\ \times (k - G\rho)^{-3/2}. \qquad (3.3)$$

A comparison of the ultimate depth of the second layer $h_2^C N_S^2(1 + R_f G\rho)^{-\frac{3}{4}}$ with $(1 - G\rho)$ is shown on Fig. 5. On a log–log plot it is seen
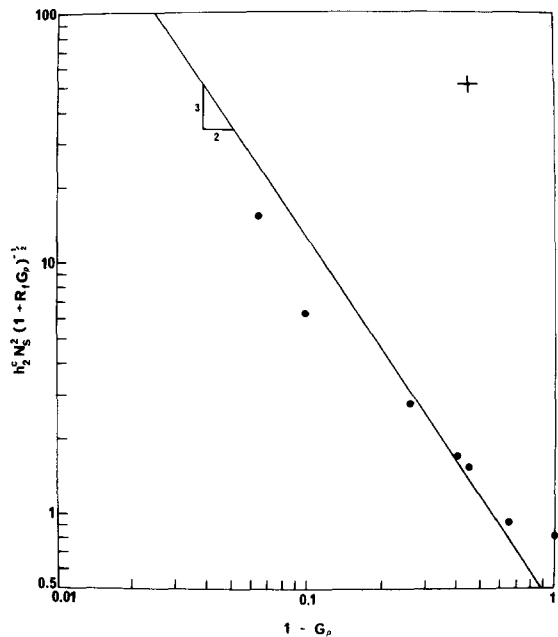
Fig. 5. A log–log plot of the depth of the second layer h_2^C multiplied by $N_S^2(1 + R_f G\rho)^{-\frac{3}{4}}$ with $R_f = 0.56$, against $1 - G\rho$. A line of slope $-\frac{3}{2}$ is drawn through the data points. The error bars estimate 90% confidence limits on the data.

that the scaling indicated by (3.3) collapses the data. A line of slope $-3/2$ as suggested by (3.3) fits the data fairly well considering all the approximations made in deriving the theoretical prediction.

It is clear that the third and subsequent layers may be dealt with in an exactly analogous way. However, this will not be done in detail here. Some remarks on their properties will be made in the next section.
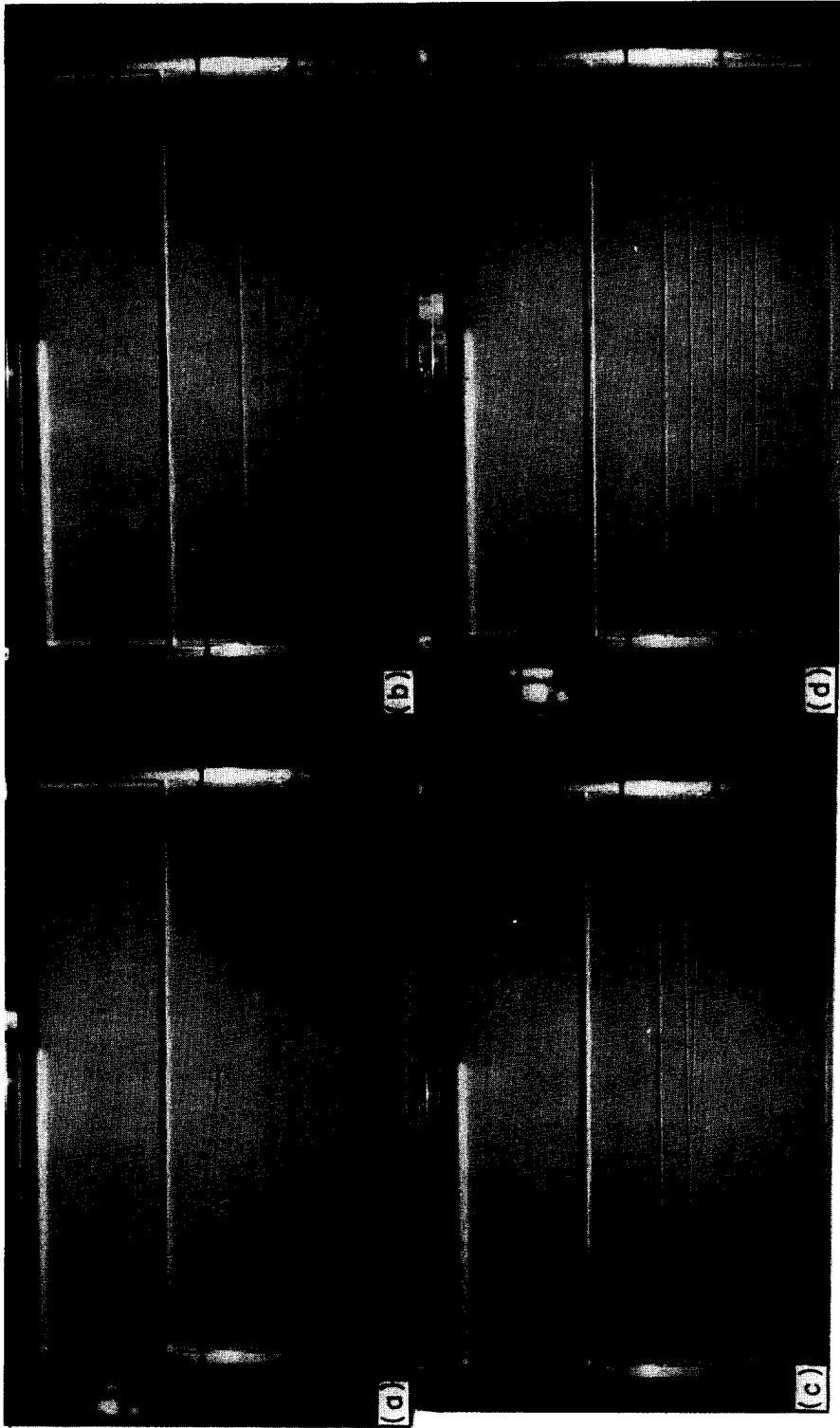
Fig. 4. These photographs show successive stages in the formation of layers by imposing a buoyancy flux at the top of opposing gradients of sugar and salt. In this run the ratio of the gradients $G\rho = 0.6$ and the photographs are taken at the following times after the addition of the upper layer. (a) 41 min. (b) 4 h 26 min, (c) 7 h 9 min, (d) 44 h 13 min.
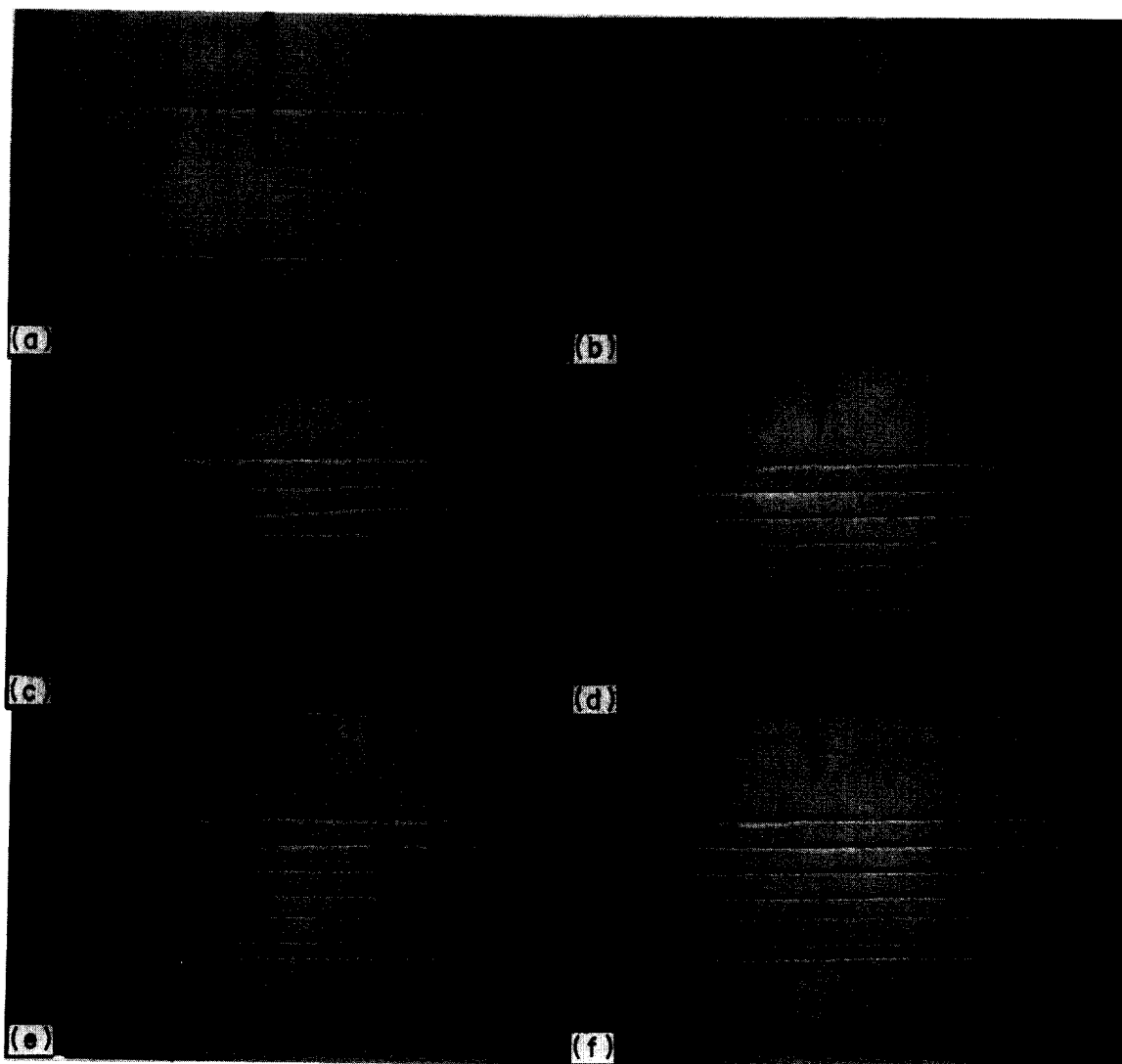
Fig. 6. A sequence of photographs showing the formation and destruction of layered sugar/salt structure in a double gradient region between two well-mixed layers. The ratio of the gradients $G\rho = 0.92$ and the steps in T and S across the outer edges of the gradient region are designed to be very small ($< 0.5^0/_{00}$). The photographs cover about 7 days, the precise times after the tank was filled being given below. The scale near the bottom of the tank is 10 cm divided into 1-cm light and dark parts. The conductivity probe is visible in the photographs. (a) 0 min, (b) 17 min, (c) 1 h 17 min, (d) 1 h 52 min, (e) 20 h 7 min, (f) 44 h 6 min, (g) 50 h 5 min, (h) 67 h 52 min, (i) 96 h 15 min, (j) 163 h 51 min.
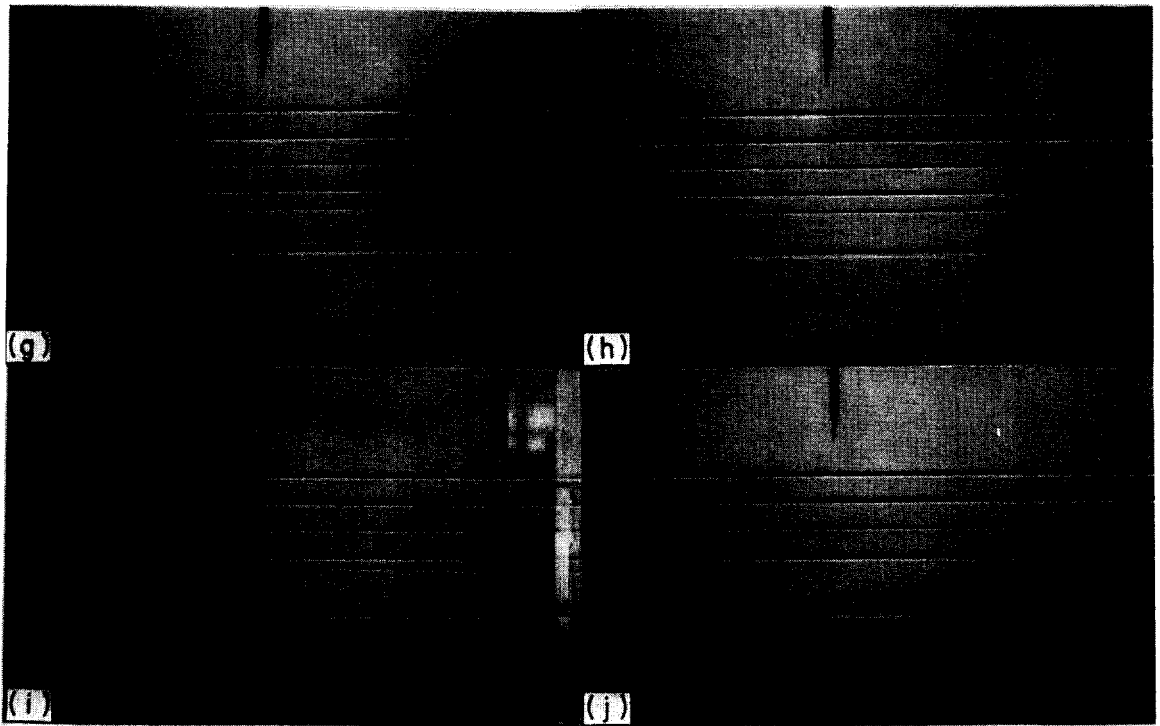
Fig. 6.
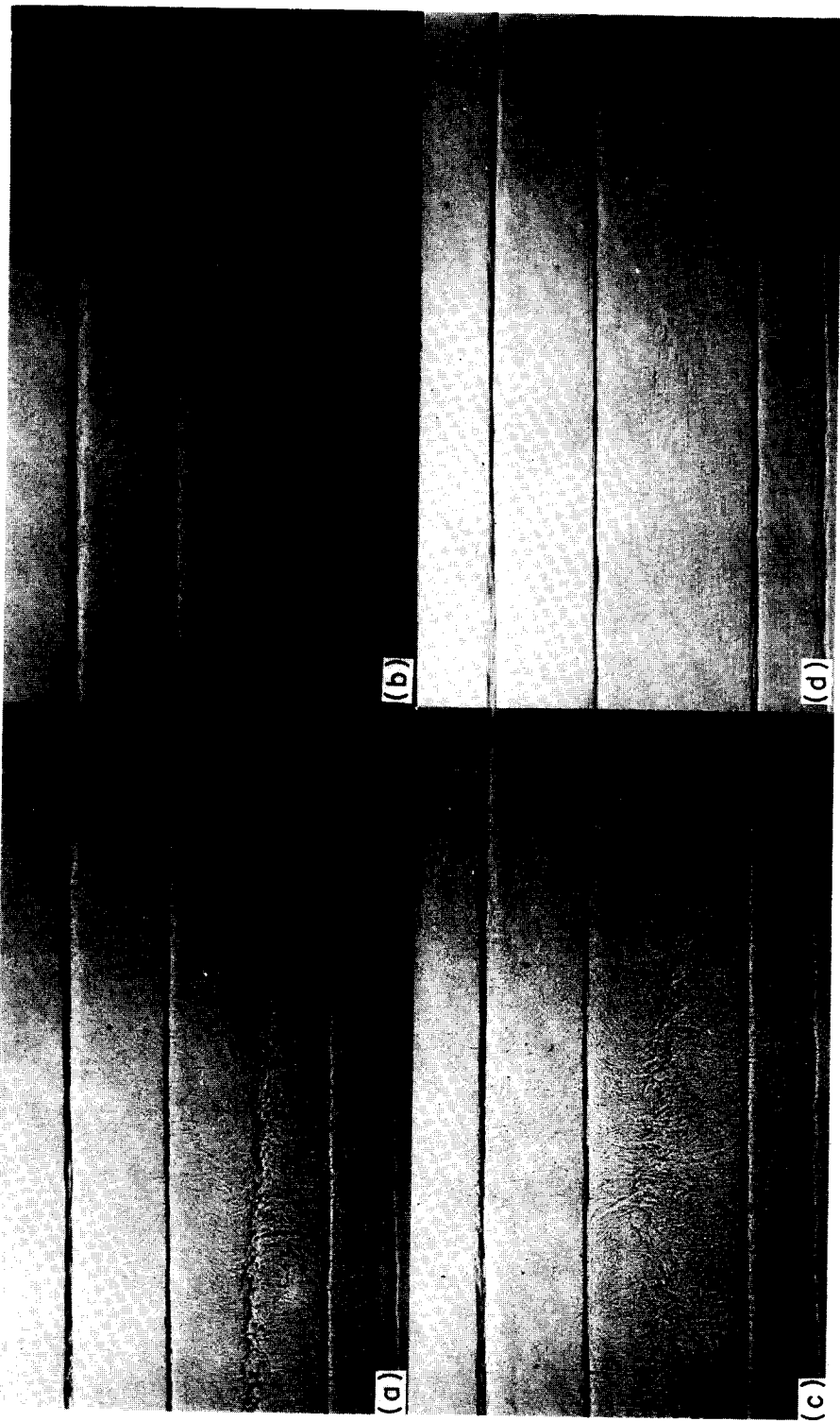
Fig. 10. A sequence taken from a time-lapse ciné film of the breakdown of an interface.

4. COMPARISON OF BOUNDARY AND INTERIOR ENERGY SOURCES

The results of Sections 2 and 3 show that as $G\rho \to k$ for fixed values of N_S and the boundary flux B_T, the size of the layers increases. The experimental results of Section 2 provide evidence that $k = 1$; in the following discussion we will take that to be the case. Consequently, in the limit as $G\rho \to k$ the density gradient of the water column becomes vanishingly small. Thus the question arises as to whether in the limit $G\rho = k$ the interior behaves like an unstratified fluid or whether the presence of the two opposing gradients of T and S play a role in the dynamics.

To examine this question note that the density gradient in the water column $d\rho/dz$ is related to the individual component gradients by the relation

$$N^2 \equiv -\frac{g}{\bar{\rho}}\frac{d\rho}{dz}$$
$$= N_S^2 + N_T^2$$
$$= N_S^2(1 - G\rho).$$

Then (2.9) can be written in the form (for constant R_f)

$$h_1^C = QB_T^{\frac{3}{4}}N^{-2}(1 + G\rho R_f)^{-\frac{1}{4}}(1 - G\rho)^{\frac{1}{4}},$$
$$= QB_T^{\frac{3}{4}}N^{-2}F(G\rho), \qquad (4.1)$$

where Q is a constant (for constant R_f and molecular properties), and

$$F(G\rho) = \left(\frac{1 - G\rho}{1 + G\rho R_f}\right)^{\frac{1}{4}}. \qquad (4.2)$$

Now we are in a position to evaluate the effects of varying B_T and $G\rho$ whilst keeping the density gradient of the water column constant. From (4.1) we see that increasing the energy source provided by the boundary flux B_T (the external energy) increases the depth of the first layer. In contrast, increasing the energy stored in the unstable T distribution (the internal energy) decreases the depth of the first layer, as from (4.2) $F(G\rho)$ is a decreasing function of $G\rho$, with $F(G\rho) \to 0$ as $G\rho \to 1$. Rather surprisingly then, the external and internal sources have opposite effects on the depth of the first layer.

The behaviour associated with the imposed flux is the same as that found in I and needs no further explanation. To see the reason for the decreasing layer depth with increasing $G\rho$ we need to go back to (2.7). Rewriting this equation we find that

$$\left|\frac{g\Delta\rho_T}{\bar{\rho}}\right| \propto N^2\frac{1 + G\rho R_f}{1 - G\rho}h_1.$$

Thus for a given density stratification N^2 and layer depth h_1 the T step at the bottom of the layer increases as $G\rho \to 1$. Consequently, the critical T Rayleigh number will be exceeded for a smaller value of h_1 and the second layer will begin to form.

A comparison of the two energy sources is provided by considering the ratio of their contributions during the formation of the first layer. If t represents the time then

$$M = -\frac{B_T t}{\frac{1}{2}N_T^2 h_1^2}, \qquad (4.3)$$

is the ratio of the external energy input to the internal energy released during the formation of the first layer [see (2.1)]. Then with (2.4) we see that

$$M = \frac{k - G\rho}{G\rho(1 + kR_f)}. \qquad (4.4)$$

Note that M is independent of the imposed flux B_T and depends only on the ratio of the two gradients in the interior of the fluid. As $G\rho \to k$ (≈ 1), and the two gradients almost compensate, the contribution from the external source diminishes to zero. As $G\rho$ decreases the external energy source becomes more important and provides the only driving force when $G\rho = 0$. This limit is the one discussed in I.

In the limit $G\rho = k$ the boundary flux provides only a small contribution and probably acts merely as a 'trigger' to motion driven almost entirely by the internal energy source. We can estimate how the 'trigger' mechanism works as follows. In the limit $G\rho = k$, the motion is driven by the internal energy [see (4.4)]. Suppose in the limit $G\rho \to k$ the boundary flux diffuses into a thin growing boundary layer which just initiates the instability. Suppose, further, that the instability sets in when the fluid in this boundary

layer is neutrally stable. Then if $N^2 = N_S^2(1 - G\rho)$ is the density gradient in the interior this condition implies that

$$B_\rho t = N_S^2(1 - G\rho)\delta^2,$$

where $\delta \propto (\kappa_T t)^{\frac{1}{2}}$ is the thickness of the diffusive boundary layer. Hence

$$B_T(1 - R_f) = cN_S^2 \kappa_T(1 - G\rho),$$

where c is a constant. Then substituting for B_T in (2.9), with $k = 1$ we find that the ultimate depth of the first layer is

$$h_1^C = \left(\frac{R_T^c v\kappa_T c^3}{4}\right)^{\frac{1}{4}} N_S^{-\frac{1}{2}}(1 + G\rho R_f)^{-\frac{1}{4}}(1 + R_f)^{-\frac{1}{4}}$$
$$\times (1 - R_f)^{-\frac{3}{4}}. \quad (4.5)$$

This implies that the depth of the layer remains finite in the limit $G\rho \to 1$. Although this argument has been applied to the first layer, (4.5) shows that the layer depth is independent of the boundary flux. Consequently, the result will hold for all layers which should, in this limit, have the same vertical scale.

5. DESTRUCTION OF FINE-STRUCTURE

So far we have dealt with the formation of layered T and S structure from smooth gradients. It has been observed in the laboratory that layers may merge (TURNER and CHEN, 1974). The ultimate result of continual merging of layers is a single layer containing uniform gradients of T and S. In this section we will investigate some aspects of this merging process.

It has been shown by HUPPERT (1971) that under certain conditions two layers may merge into one as a result of their T and S properties becoming the same. His theoretical analysis was restricted to the case where the interfaces between the layers remained stationary. Here we report some examples of merging layers as observed in experiments with a diffusive configuration. We observed two types of merging identified either by the presence or absence of vertical migration of the interface between the two merging layers. We will treat each case in turn.

a. Moving interfaces

Most of the merging which was observed occurred as a result of an interface moving vertically until it reached an adjacent one, thereby destroying the layer in between. An example of this phenomenon is shown on Fig. 6. This series of photographs shows the formation and destruction of layers from a double gradient (the details of the experimental configuration are given in the caption) covering a period of 6 days. In this case, unlike that of the runs described in Sections 2 and 3, the flux into the system is small and merely triggers the energy release from the nearly compensating double gradients. Note that from the irregular formation process a set of six regular well-mixed layers separated by sharp interfaces is formed (Fig. 6d). The uniform thickness of the layered structure is in agreement with the ideas discussed in Section 4 for the limit $G\rho \to 1$.

Of main interest here is the subsequent layer merging as exhibited on Figs. 6(e) to (j). The interface separating the bottom two layers moves downwards [Figs. 6(e), (f), (g)] until the lower layer finally disappears [Fig. 6(h)]. The interface at the top of the lower layer now begins to move upwards and finally merges with the one above leaving four layers from the original six. These layers then remained unchanged in size for a further 2 weeks when the tank was emptied.

In order to study this case further, the output from the conductivity probe (visible in the photographs) which was driven downwards through the layers was recorded. Figure 7 shows the output of the probe as it was traversed downwards through the layers. This profile was taken at a time roughly corresponding to the profile shown in Fig. 6(f). The six layers are labelled from the top down 1 to 6. The conductivity–depth profile shows the layers to be well-mixed and separated by relatively thin interfaces. Profiles (converted to T density units by calibration) covering a period of 86 h, from the state shown in Fig. 6(h) to that in Fig. 6(j) are shown in Fig. 8. This figure shows an expansion of four profiles such as those shown in Fig. 7 with every 5th data point represented (both the depth and density scales have arbitrary
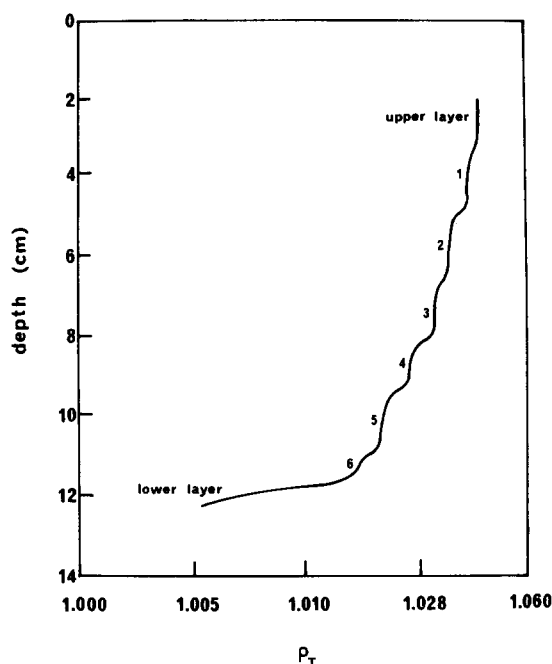
Fig. 7. A conductivity-depth profile taken through the six layers shown on Fig. 6(f). The numbers on the profile indicate the layers numbering down from the top.

Fig. 8. An expanded version of 4 profiles through the three layers 3, 4 and 5 as they merge into two layers. The points represent every 5th data point taken from profiles such as those shown in Fig. 7. The number at the bottom of each profile is the time in hours elapsed since the first profile shown was made.

origins) for the layers 3, 4 and 5. The profiles are shifted to the right on the T-axis as time increases as a result of transport of T down from above through the layers. By following the progression from profile to profile and ignoring the transport of T from above, the way in which layer 4 disappears by the upward movement of the interface beneath it is revealed.

A comparison of the profiles between 0 and 42 h shows that the interface between 3 and 4 is unchanged but that there is a relative accumulation of T in layer 5 and a slight thickening of the interface between layers 4 and 5. Between 42 and 55 h the interface between layers 4 and 5 has moved vertically some 0.35 cm. Consequently, the value of T at 3.0 cm decreases as the interface rises whilst the value of T in layer 5 increases. Superposition of the two profiles at 42 and 55 h shows that the increase in T in layer 5 is almost the same as that lost from the interface region (between 2.6 and 3.6 cm) as the interface rises.

There is also a general smearing out of layer 4 during this time. The fourth profile taken at 86 h shows that the interface has now moved right up to layer 3 and no evidence of the intermediate layer remains. Superimposing the profiles taken at 0 and 86 h we see that they fit closely from 0 to 2.5 cm (the original centre of layer 4) but that there has been an enhanced transport of T into the region 2.5 to 5.0 cm. The effect of removing the middle layer 4 has been to increase the transport of T downwards.

Samples were withdrawn from the centres of the layers for each run and the refractive index measured. Using these samples and the output from the conductivity probe it is possible to estimate the sugar and salt content of each layer. The results of these calculations are shown in Table 1.

Before suggesting an explanation of this phenomenon we will present a case where the position of an interface was measured as a function of time. This is shown in Fig. 9. The experiment
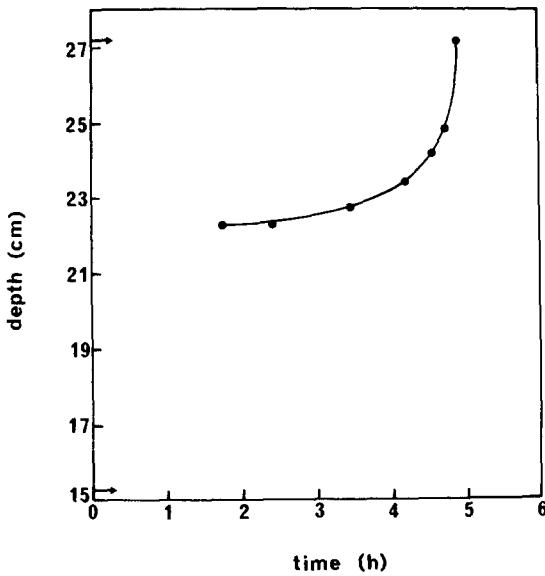
Fig. 9. The position of the central interface plotted against the time elapsed since the system was set up. The two marks on the y-axis indicate the positions of the interfaces on either side of the one under consideration. The configuration for this experiment was in the 'finger' sense in sugar/salt.

Table 1. The T and S properties of layers 3, 4 and 5 measured during the merging of layers 4 and 5

Profile	Layer	ρ_{salt}	ρ_{sugar}	$\alpha\Delta T$ ‰	$\beta\Delta S$ ‰	$R\rho = \dfrac{\beta\Delta S}{\alpha\Delta T}$
0 h	3	0.031	0.017	4	6	1.5
	4	0.027	0.023	5	6	1.2
	5	0.022	0.029			
42 h	3	0.033	0.017	5	6	1.2
	4	0.028	0.023	1	7	7.0
	5	0.027	0.030			
55 h	3	0.033	0.018	5	12	2.4
	5	0.028	0.030			
86 h	3	0.034	0.021	5	10	2.0
	5	0.029	0.031			

from which these data are taken was carried out by Prof. J. S. Turner. The feature to note is that the motion of the central interface is initially quite slow but becomes very rapid as it approaches the upper interface. These measurements were made in a finger configuration. However, apart from

accelerating the merging the gross features are essentially the same as for a diffusive interface.

There is evidence (see LINDEN and SHIRTCLIFFE, 1977) that when fluxes of T and S are imposed at the top and bottom of two layers separated by a diffusive interface, it is not always possible for the interface to transmit these imposed fluxes. As a result, there may exist an imbalance between the two sides of the interface causing it to move. A physical mechanism for this motion exists when the two layers on either side of the interface have different depths. In a convecting layer, the velocity scale of the motions driven by a given buoyancy flux increases as the depth of the layer increases. Motions in a layer adjacent to a density interface tend to erode that interface (CRAPPER and LINDEN, 1974). Consequently, the erosion on the side of the deeper layer will be more vigorous, tending to increase the depth of the layer at the expense of the shallower one.

The result of this mechanism will have two characteristics. First, the interface would always move in one direction and it would move so that the shallower of the two layers became even shallower. Second, the rate at which the interface moved would increase as the imbalance in the layer depths, and, therefore, the imbalance in the velocities in the layers, increased.

The first characteristic is evident in the interface motions shown in Fig. 6. In Figs. 6(e) to (g) the bottom layer is lost as the interface moves downwards; initially the layer above the interface was slightly deeper. In Figs. 6(h) to (j) the situation is reversed. Now the bottom layer is deeper than the one above and the interface moves upwards until the latter is removed. A comparison of the profiles taken at 55 and 86 h (Fig. 8) also shows the erosion of the interface from below. The fact that the remaining four layers now remain unchanged is probably because the fluxes are so small that there is insufficient energy left to erode the remaining interfaces.

The second characteristic is exhibited by the plot of interface position with time shown on Fig. 9. The motion is slow to begin with, when there is little difference in the layer depths. As the difference in the layer depths increases the

interface moves more rapidly, showing the unstable nature of the system.

b. *Stationary interfaces*

Layer merging brought about by the destruction of a stationary interface is more difficult to document. This is partly because it appeared to be more infrequent than in the case where the interfaces moved, and partly because it occurred more rapidly. However, several cases were observed and we report the general features below.

An example of this kind of breakdown can be found in Fig. 6(d). In the middle of the bottom layer, particularly on the right-hand side, the destruction of an interface is occurring. This case exhibits most of the features that seem to be characteristic of the destruction of a stationary interface. Firstly, it seems to be two-dimensional. Note that on the right there is quite a sharp interface which becomes progressively thicker to the left. Secondly, the breakdown is characterized by the interface becoming fuzzy and quite thick. Thirdly, no interface which settled down to the sharp form as shown by the other interfaces on that photograph was observed to break down in this way.

A better example is provided by Fig. 10 which is a series of stills taken from a time-lapse ciné film of the break-up of an interface. Initially, a single layer was formed in the double gradient region, in the manner described in Section 2. Subsequently, a second layer and then a third formed beneath the first. The interface between these two layers never became sharp and was constantly reacting to bombardment from blobs released from the top of the second layer. This was seen very clearly in the time-lapse film. As the experiment progressed horizontal motions began in the second layer and the interface would tilt away from the horizontal. Eventually, the interface became very fuzzy and broke down with large-scale, rapid, horizontal motions occurring in the whole region occupied by the second and third layers.

These observations provide some support for HUPPERT'S (1971) theory of the merging of layers in such a system. He predicted that when the ratio of the T and S fluxes across an interface was not constant with changes in the density ratio $R\rho$ (the 'variable regime'), the properties of the two layers on either side of the interface would approach each other and the interface separating them would be removed. No observations of sugar/salt diffusive interfaces (LINDEN and SHIRTCLIFFE, 1977) have provided any evidence of such a 'variable regime', and so it would be expected that the system be stable. On the other hand, LINDEN (1974) has shown that entrainment across an interface changes the flux ratio. From the ciné film there was evidence that the bombardment of the interface by blobs from above was causing entrainment. Hence, it is possible, although by no means certain, that this entrainment may have been responsible for putting this interface into a 'variable regime' and (by Huppert's theory) making the system unstable.

6. DISCUSSION

We have discussed some ways in which layers may be formed or destroyed by double-diffusive processes. Attention has been focussed on one-dimensional processes and on 'diffusive' convection. However, many of the bulk features, such as the existence of relatively thin interfaces separating convecting layers driven by an unstable buoyancy flux across the interface, characteristic of diffusive convection, have also been found in 'finger' convection (STERN and TURNER, 1969). As these bulk properties, and not the details of the mechanisms, appear to be responsible for the generation of fine-structure, it is expected that much that has been said above in the 'diffusive' context will be applicable, qualitatively at least, to the 'finger' case.

Layers were formed by imposing a vertical buoyancy flux across the horizontal boundaries of a fluid region containing opposing gradients of two components. It was found that the scale of the layers depends on both the magnitude of the imposed buoyancy flux and the ratio of the contributions to the density of the two components $G\rho$. The fraction of the total energy used to produce the layers drawn from the unstable T distribution in the interior is found to depend

only on $G\rho$. In the limit as $G\rho \to 1$ when the two gradients almost cancel, all the energy is drawn from the interior, the boundary flux acting only as a trigger to initiate the motion. It is suggested in this limit that all the layers formed will be of equal size.

The conditions under which layers merge were also examined. The most commonly observed mechanism was the vertical migration of an interface until it reached a neighbouring one thereby removing the layer between. In other circumstances the interface remained at the same vertical position and was observed to become fuzzy and eventually to break down. The causes of these types of breakdown are not well understood although we have provided plausible explanations for both.

It was mentioned at the beginning of this paper that the primary motivation of this study is a desire to understand observations of oceanic fine-structure which exhibit the features of layering. On the other hand, it is clear that the experiments described above are very restricted and the extrapolation to the oceanic context is not a trivial one. It is instructive, though, to attempt to make some comparisons with oceanographic data, if for no other reason than to define more clearly the inadequacies of the laboratory simulations. At best such a comparison will be semi-quantitative because the precise quantitative effect of the different molecular properties of the laboratory and oceanic components is not known.

A region which has proven to be rich in fine-structure and which has received considerable attention over the past few years is in the northeast Atlantic where the Mediterranean water flows westward after passing through the Straits of Gibraltar. As a result of high evaporation the Mediterranean water is warm and saline compared with the Atlantic water, and its high salinity core can be traced across the Atlantic. We are concerned here with a region approximately 34 °N, 12 °W where the depth of this core is observed to be about 1200 m. Underneath this core, to a depth of about 1800 m, layers have been observed (TAIT and HOWE, 1971). Recently, WILLIAMS (1974) has observed salt fingers in this region of layering, showing that double-diffusive convection is active in this area. Tait and Howe's data show some 20 layers, and the ratio of the mean density gradients of heat and salt at that time were $G\rho \approx 0.9$. Thus (4.4) indicates that the energy in the mean unstable salt distribution could provide 85% of the total energy required to re-establish these layers provided these mean gradients are maintained as the system runs down. Consequently, only a relatively small input of boundary flux from a fresh influx of Mediterranean water into the area would be required to reform the layers. It is expected as described in Section 4, for this large value of $G\rho$ that the layers would be approximately the same size. This is indeed observed to be the case, the only appreciable change in scale being at the bottom of the region where the layers become thinner.

A situation where the layering can justifiably be attributed to one-dimensional formation is provided by hot brine pools at the bottom of the Red Sea. Measurements of temperature and salinity show a pronounced layered structure, and recent echosounder data taken in the Atlantis II Deep (SCHOELL, 1974) show up to 9 layers of varying thickness. Mean salinity and temperature gradients put $G\rho \lesssim 0.1$ (TURNER, 1969) which means that the energy required for the layering is almost entirely provided by the boundary flux: in this case a geothermal heat flux of order $10\,\mu\mathrm{cal\,cm}^{-2}\,\mathrm{s}^{-1}$. The echosounder traces show that the scale of the layers varies with depth, becoming smaller the further the layer is from the source of the boundary flux. This is expected for such a low value of $G\rho$.

Observations have also been made of layers in the Tyrrhenian Sea, which were first discovered in 1970 (JOHANNESSEN and LEE, 1974). These layers appear to be quite persistent and have horizontal scales up to 140 km. The vertical scale of these layers varies from 10 to 20 m at 600 m depth to about 200 m below 1100 m. At the shallower depths (600 to 1000 m) $G\rho \approx 0.7$ whilst $G\rho$ is very close to unity below 1000 m. Thus the increase in the scale of the layers with depth is consistent with the laboratory observation that the scale of the layers increases as $G\rho \to 1$.

The qualitative agreement between these oceanographic examples and the laboratory experiments is encouraging. However, the oceanic data are not sufficiently detailed to provide a stringent test for the model of layer formation. It is doubtful whether the layers observed in the Tyrrhenian Sea or beneath the Mediterranean water can be described solely by a one-dimensional process. The former layers appear to exist only above the deeper parts of the basin which may be a result of the effects of bottom topography. In the case of the Mediterranean water there sometimes appear to be discontinuities in the layers (ELLIOT, HOWE and TAIT, 1974) which indicate a lack of horizontal uniformity in the formation process. This non-uniformity may be indicative of the early stages of layer formation (see Fig. 6c) but is more likely to be a result of two-dimensional effects.

REFERENCES

CRAPPER P. F. and P. F. LINDEN (1974) The structure of turbulent density interfaces. *Journal of Fluid Mechanics*, **65**, 45–63.

ELLIOT A. J., M. R. HOWE and R. I. TAIT (1974) The lateral coherence of a system of thermo-haline layers in the deep ocean. *Deep-Sea Research*, **21**, 95–107.

HUPPERT H. E. (1971) On the stability of a series of double-diffusive layers. *Deep-Sea Research*, **18**, 1005–1021.

HUPPERT H. E. and J. S. TURNER (1972) Double-diffusive convection and its implications for the temperature and salinity structure of the ocean and Lake Vanda. *Journal of Physical Oceanography*, **2**, 456–461.

JOHANNESSEN O. M. and O. S. LEE (1974) A deep stepped thermo-haline structure in the Mediterranean. *Deep-Sea Research*, **21**, 629–639.

LINDEN P. F. (1974) A note on the transport across a diffusive interface. *Deep-Sea Research*, **21**, 283–287.

LINDEN P. F. and T. G. L. SHIRTCLIFFE (1977) The diffusive interface in double-diffusive convection. *Journal of Fluid Mechanics*, sub judice.

NESHYBA S., V. T. NEAL and W. DENNER (1971) Temperature and conductivity measurements under Ice Island T-3. *Journal of Geophysical Research*, **76**, 8107–8120.

OSTER G. (1965) Density gradients. *Scientific American*, **213**, 70–76.

SCHOELL M. (1974) *Valdivia VA 01/03 Rotes Meer-Golf von Aden. Hydrographic* II. Bundesanstalt fur Bodenforschung, Hannover.

SHIRTCLIFFE T. G. L. (1973) Transport and profile measurements of the diffusive interface in double diffusive convection. *Journal of Fluid Mechanics*, **57**, 27–43.

STERN M. E. and J. S. TURNER (1969) Salt fingers and convecting layers. *Deep-Sea Research*, **16**, 497–511.

TAIT R. I. and M. R. HOWE (1971) Thermohaline staircase. *Nature*, **231**, 178–179.

TURNER J. S. (1965) The coupled turbulent transports of salt and heat across a sharp density interface. *International Journal of Heat and Mass Transfer*, **8**, 759–767.

TURNER J. S. (1967) Salt fingers across a density interface. *Deep-Sea Research*, **14**, 599–611.

TURNER J. S. (1968) The behaviour of a stable salinity gradient heated from below. *Journal of Fluid Mechanics*, **33**, 183–200.

TURNER J. S. (1969). A physical interpretation of the observations of hot brine layers in the Red Sea. In *Hot brines and recent heavy metal deposits in the Red Sea*, E. T. DEGENS and D. A. ROSS, editors, Springer-Verlag, pp. 164–173.

TURNER J. S. (1973) *Buoyancy effects in fluids*, Cambridge University Press, 367 pp.

TURNER J. S. and C. F. CHEN (1974) Two-dimensional effects in double-diffusive convection. *Journal of Fluid Mechanics*, **64**, 577–592.

VERONIS G. (1965) On finite amplitude instability in thermohaline convection. *Journal of Marine Research*, **23**, 1–17.

WILLIAMS A. J. (1974) Salt fingers observed in the Mediterranean outflow. *Science*, **185**, 941–943.

APPENDIX 1: THE EXPERIMENTAL METHOD

To set up the opposing gradients of T and S required for these experiments, the double-bucket method described by OSTER (1965), modified in the manner of TURNER and CHEN (1974) was used. The tank measured 10 cm wide, 61 cm long and 46 cm deep.

For the experiments described in Sections 2 and 3, a double gradient region about 27 cm deep was produced, this process taking about 45 min. Care was taken to ensure that the solutions were at room temperature, and at no stage was there evidence of instabilities occurring in the interior of the fluid which could not be traced back to the boundary fluxes. Once the double gradient region was set up, a uniform layer was added on top. In every case the density step in sugar was 0.030 ± 0.0005 g ml^{-1} and the density step in salt 0.029 ± 0.0005 g ml^{-1} relative to the values at the top of the gradient region, with the net stable density step between the layer and the gradient region always less than 0.0015 g ml^{-1}. A range of S gradients were used with N_S^2 taking values between 0.36 and 4.1 rad s^{-1}. The ratio of the gradients $G\rho$ was varied between 0 and 0.96. Using such large steps of sugar and salt at the top of the gradient region, it was intended to provide reasonably constant fluxes across the top boundary, at least during the formation of the first layer. In every case the initial step in $\binom{T}{S}$ was at least 5 times as large as

$$\frac{\mathrm{d}\rho\binom{T}{S}}{\mathrm{d}z} h_1^c .$$

The motions were visualized using a shadowgraph and use was made of both still and time-lapse photography. The depths of the layers were measured at various times during the experi-

ments, both directly from the shadowgraph screen and from the photographs. During the early stages of the formation of a layer, the depth could not be determined very accurately, but once the interface had sharpened it was measured to within 0.1 cm.

For the experiments described in Section 5 a different initial stratification was used. Two well-mixed layers were set up separated by a double-gradient region. The depths of the upper and lower layers were 12.4 and 12.1 cm, respectively, whilst the depth of the double gradient region was 12.5 cm. The lower layer initially contained no salt, but had a density of $1.053\,g\,ml^{-1}$ due to dissolved sugar. In the gradient region the sugar concentration decreased uniformly to zero at the top whilst the salt concentration increased uniformly to the upper layer value, making the density of that layer $1.049\,g\,ml^{-1}$. This system was monitored visually with a shadowgraph and with a conductivity probe (see CRAPPER and LINDEN, 1974) at various times over a 7-day period. One-millilitre samples were also withdrawn at certain depths at various times during the experiment. The refractive indices of these samples were measured and, from calibration used in conjunction with the conductivity probe, allowed the sugar and salt concentrations (in density units) to be determined in the layers which formed. The conductivity probe was traversed vertically through the fluid to give profiles of the salt distribution in the vertical. From calibration it was found that the output from the conductivity probe was virtually independent of the sugar concentration for values less than 3% more dense than pure water. It was found by this method to be able to measure the salt contribution to the density to better than $0.001\,g\,ml^{-1}$ and the sugar contribution to better than $0.002\,g\,ml^{-1}$.

APPENDIX 2: THE CONDITION FOR THE ONSET OF CONVECTION IN THE SECOND LAYER

The mechanism by which convection is initiated ahead of the growing first layer is assumed to be that proposed by TURNER (1968) for the case of a stable salinity gradient heated from below. In essence, the faster diffusing T component diffuses ahead of the growing layer producing an unstable boundary layer ahead of the interface. Both the boundary layer thickness and the T-step across it increase with time until it becomes unstable thereby initiating the convection.

The analysis follows that of I (Section 3) almost exactly, with only minor modification to allow for the presence of the second gradient in the interior. Consequently, the description here will be brief.

Suppose the interface is moving with velocity

$$w = ct^{-\frac{1}{2}}, \qquad (A1)$$

as indicated by (2.4). It is shown in I that, in the limit $c^2/\kappa_T \gg 1$ the T distribution at time t is given by

$$T = At^{\frac{1}{2}}\exp(-cz/\kappa_T t^{\frac{1}{2}}), \qquad (A2)$$

where $T = At^{\frac{1}{2}}$ on the interface and z is now the distance ahead of the moving interface. A convenient measure of the boundary layer thickness δ_T is

$$\delta_T \equiv 2\Delta T / \left|\frac{\partial T}{\partial z}\right|_{z=0}.$$

Then (A2) implies

$$\frac{\delta_T}{h_1} = \frac{2\kappa_T t^{\frac{1}{2}}}{ch_1},$$

$$= \kappa_T/c^2,$$

by (A1). Identification of c from (A1) and (2.4) give

$$\frac{\delta_T}{h_1} = 2\kappa_T B_T^{-1} N_S^2 (1 + kR_f)^{-1}(k - G\rho). \qquad (A3)$$

The effect of the second gradient is apparent from the last term on the right-hand side of (A3).

Finally, we need to establish a criterion for the breakdown of this boundary layer. Again following I, we apply the result of linear stability analysis for constant gradients of T and S found by VERONIS (1965). Although taken out of context this will give a qualitative estimate of the breakdown criterion. Veronis' result is that when R_T (the T Rayleigh number) exceeds a critical value then the system will be unstable to an infinitesimal disturbance. This critical value is related to the S Rayleigh number R_S by the relation

$$R_T = \frac{v}{v + \kappa_T}R_S + \frac{27\pi^4}{4}. \qquad (A4)$$

We apply the result to the present situation by defining the Rayleigh numbers in terms of the T and S boundary layer parameters, i.e.

$$R\binom{T}{S} = \left|\frac{g\Delta\rho\binom{T}{S}}{\bar{\rho}}\right| \frac{\delta^3\binom{T}{S}}{v\kappa_T}. \qquad (A5)$$

Then (A4) can be written as

$$R_T\left\{1 - \frac{|\Delta\rho_S|}{|\Delta\rho_T|}\left(\frac{\delta_S}{\delta_T}\right)^3\right\} = \frac{27\pi^4}{4} - \frac{1}{\sigma+1}R_S. \qquad (A6)$$

As the boundary layers δ_S and δ_T are formed by diffusion

$$\frac{\delta_S}{\delta_T} \propto \left(\frac{\kappa_S}{\kappa_T}\right)^{\frac{1}{2}}.$$

Typically, convection sets in for values of $R_S \lesssim 10^4$; for sugar and salt $\sigma \equiv v/\kappa_T \approx 10^3$, and so we can neglect the second term on the right-hand side of (A6). Use of (2.3) in (A6) gives as an estimate of the critical T Rayleigh number

$$R_T^C \doteqdot \frac{27\pi^4}{4}\left[1 - k\left(\frac{\kappa_S}{\kappa_T}\right)^{3/2}\right]^{-1}. \qquad (A7)$$

Taking $k = 1$ and giving κ_S and κ_T the values appropriate for sugar and salt we find $R_T^C \doteqdot 531$.